Tissue and Cell 78 (2022) 101893

Contents lists available at ScienceDirect

Tissue and Cell

journal homepage: www.elsevier.com/locate/tice

Dynamic cytosolic foci of DPPA4 in human pluripotent stem cells

Raed Abu-Dawud [a,b,*], Bhavesh V. Mistry [a], Renad Almahdali [c,d], Maryam M. Matin [e], Ayodele Alaiya [f], Fatimah Alghamdi [g], Hala Alamari [g], Nadya Al-Yacoub [a], Junaid Kashir [a,h,j], Marwa Houssein [a,i,k], Abdullah Alawad [g,**], Peter W. Andrews [b], Abdullah M. Assiri [a,h]

[a] Department of Comparative Medicine, King Faisal Specialist Hospital & Research Centre, 11211 Riyadh, Saudi Arabia
[b] Centre for Stem Cell Biology, University of Sheffield, Department of Biomedical Science, S10 2TN Sheffield, UK
[c] King Salman Humanitarian Aid and Relief Centre, Volunteer Programs Department. King Abdullah Rd., King Saud University, Riyadh 12371
[d] College of Science and General Studies, Alfaisal University, 11533 Riyadh, Saudi Arabia
[e] Department of Biology and Institute of Biotechnology, Ferdowsi University of Mashhad, 9177948974 Mashhad, Iran
[f] Department of Stem Cell & Tissue Re-Engineering, King Faisal Specialist Hospital & Research Centre, 11211 Riyadh, Saudi Arabia
[g] National Center for Biotechnology, Life Science and Environment Research Institute, King Abdulaziz City for Science and Technology, 12354 Riyadh, Saudi Arabia
[h] College of Medicine, Alfaisal University, 11533 Riyadh, Saudi Arabia
[i] Department of Biological Science, Beirut Arab University, Beirut, Lebanon
[j] Department of Biology, College of Arts and Sciences, Khalifa University, Abu Dhabi, United Arab Emirates
[k] Department of General Sciences and English Language, College of Applied Sciences, Al Maarefa University, Riyadh, Saudi Arabia

ARTICLE INFO

Keywords:
DPPA4
Cytosolic
Nuclear
Shuttling
Pluripotent stem cells
Self-renewal

ABSTRACT

DPPA4 is essential for the pluripotent stem cell state, yet its function is poorly understood. DPPA4 is localized in the nucleus, where it is associated with active chromatin. We now report that it is also present in the cytosol, where it appears as diffused clouds, distinct foci and sometimes as spaghetti-like structures. This cytosolic localization is dynamic and DPPA4 shuttles between the cytosol and the nucleus. Its presence is almost abolished from the nucleus upon differentiation. Co-immunoprecipitation studies highlighted novel protein interactors, many of which are also found in the cytosol and are implicated in mRNA processing and RNA and protein transport between the cytosol and the nucleus. Finally, the depletion of *DPPA4* resulted in cytosolic accumulation of vesicles. The cytosolic presence of DPPA4 highlights unexplored research directions that could significantly advance the understanding of DPPA4 in pluripotent stem cells and in cancer.

1. Introduction

DPPA4 (Developmental Pluripotency Associated Factor 4) is essential for the pluripotent stem cell state, and its re-activation is required for the reprogramming of somatic cells into induced pluripotent stem cells (iPSC) (Bortvin et al., 2003; Ivanova et al., 2006; Enver et al., 2005; Golipour et al., 2012; Hernandez et al., 2018). The utilization of patient specific iPSCs is a very promising approach to treat degenerative diseases like Parkinson's, Alzheimer's, Diabetes mellitus, etc., but requires their detailed understanding to ensure patient safety, and the development of efficient reprogramming and efficient differentiation protocols. Key pluripotency factors like *OCT3/4*, *SOX2* and *NANOG* maintain the expression of pluripotency genetic core circuits and self-renewal (Niwa et al., 2000; Chambers et al., 2003; Mitsui et al., 2003; Ying et al., 2003; Boyer et al., 2005). Upon depletion, genetic core circuits are silenced, and self-renewal is exited. DPPA4, however, exits only self-renewal, without affecting expression of the genetic core circuits (Ivanova et al., 2006; Enver et al., 2005; Niwa et al., 2000; Chambers et al., 2003; Mitsui et al., 2003; Matin et al., 2004). This uncoupling mechanism remains unknown and might be due to the affiliation of DPPA4 to an entirely different protein class (Aravind and Koonin, 2000), unlike most other known key players, which are mainly transcription factors or signalling components, reviewed by Loh and Lim (Loh and Lim, 2011). DPPA4 is a SAP (SAF-A/B, Acinus and PIAS) domain protein, a putative DNA binding domain, mainly found in proteins of chromosomal architecture, DNA repair and (pre)-mRNA metabolism, most of which occupy

* Correspondence to: King Faisal Specialist Hospital & Research Center, Department of Comparative Medicine, MBC 03, P.O. Box 3354, Riyadh 11211, Saudi Arabia.
** Corresponding author.
E-mail addresses: rabudawud@kfshrc.edu.sa (R. Abu-Dawud), alawad@kacst.edu.sa (A. Alawad).

https://doi.org/10.1016/j.tice.2022.101893
Received 5 June 2022; Received in revised form 28 July 2022; Accepted 6 August 2022
Available online 9 August 2022

nuclear roles (Aravind and Koonin, 2000). Indeed, *DPPA4* is localized in the nucleus, where it binds to and activates preferentially enhancer regions of pluripotent stem cell genes, in particular H3K4, while suppressing the expression of somatic genes (Hernandez et al., 2018; Engelen et al., 2015; Masaki et al., 2007, 2010). DPPA4 maintains an open chromatin state via H2AX and Parp1 (Hernandez et al., 2018). Although DPPA4 is a SAP domain protein, which are known to bind AT-rich sequences (Aravind and Koonin, 2000), DPPA4 was reported to bind preferentially GC-rich regions by which it supports the activity of essential pluripotency pathways such as WNT, TGFß, and PI3K-Akt signalling (Li et al., 2020). Taken together, it is thought that DPPA4 is operative only in the nucleus, but here we show that DPPA4 is dynamically trafficking within the cytosol, and shuttling between the cytosol and the nucleus, and decreases dramatically in the nucleus upon differentiation. These insights bring the cytosol into the spotlight of future DPPA4 investigations.

2. Materials and methods

2.1. Cell Culture

Human embryonic stem cells line H7 (Thomson et al., 1998) and induced pluripotent stem cell line IMR90–4 (Yu et al., 2007) were grown in mTeSR, E8 or in Knockout-DMEM (supplemented with 20 % Knockout-Serum Replacement (Invitrogen), 1x non-essential amino acids, 1 mM glutamine, 0.1 mM β-mercaptoethanol and 8 ng/ml bFGF (Invitrogen)) seeded on matrigel (BD Bioscience). The cells were cultured at 37 °C under a humidified atmosphere of 5 % CO_2 in air and passaged every 3–5 days using collagenase type IV (Invitrogen) by scraping with glass-beads (Sigma). Human embryonal carcinoma NTERA2 cl. D1 (Andrews et al., 1984) and 2102Ep (Andrews et al., 1980) were cultured in DMEM supplemented with 10 % FCS and 1 mM glutamine at 37 °C in a humidified atmosphere of 10 % CO_2 in air and passaged using trypsin.

2.2. Retinoic Acid (RA) mediated differentiation

All-*trans*-retinoic Acid 10^{-5} M (Sigma Aldrich) was added to a half confluent flask and cultured further in the presence of retinoic acid (RA) until harvested.

2.3. Engineering the DPPA4-EGFP fusion construct

The N-terminus of EGFP was fused to the C-terminus of DPPA4. For this purpose the pGEM-T-DPPA4 construct was used as a template. For in frame fusion, the reverse primer (5′ –CTTACCGGTGATTCCC ATTGGAGGCTTTTTATTAAGAC- 3′) was designed such that it inserted two base pairs in order to maintain the reading frame and it deletes the STOP-codon of *DPPA4* while inserting the restriction site *Age*I. The forward primer (5′- CCGCTCGAGGGCC ATTTTGGAAGCATGTTGC - 3′) carries an *Xho*I restriction site. The resulting *DPPA4* amplicon was inserted into the pCAG-EGFP vector, which was previously digested with *Xho*I and *Age*I, and subsequently sequenced.

2.4. Transfection of hESCs and hECCs with plasmid DNA or siRNA

A 70% confluent well of a 6-well plate was transfected using Lipofectamine2000 (Invitrogen) according to the standard manufacturers protocol. siRNA sequences: *DPPA4:* DPPA4-A: 5′ - AAGAGGAUCAGCAGGCUUCUA - 3′; DPPA4-B: 5′ - AAUUGCUUUGCCAGGAACAUC - 3′; *OK(a)*: 5′ – GAGCAGGUUCU UCGUGAGU UC - 3′.

2.5. Imaging

Immunofluorescence and time-laps images (over night every 12 −15 min in incubation chamber) were taken using the EVOS (LifeTechnologies) imaging system.

2.6. Peptide sequences for DPPA4-antisera

Production of DPPA4 antibodies was outsourced to GenScript (USA), AB1 and AB2, and Eurogentec (Belgium) (AB3 and AB4). AB1 =REEDQQASNQPNS, for AB2 =AEHTDNPRPQKKIP, AB3 and AB4 both peptides were mixed.

2.7. Immunostaining

Cells were fixed using 4 % paraformaldehyde for 15 min at RT. Then cells were washed 3 times in PBS before adding PBST (0.1 % Triton X-100) for permeabilization for 20 min at RT followed by 3 washes with PBS. Then blocking buffer (10 % goat serum in PBS) was added for 1 h at RT. After blocking, primary customized DPPA4 antibody was added (diluted 1:100 or 1:400) in 5 % goat serum overnight at 4 °C followed by 3 washes with PBS. Subsequently, a goat anti-rabbit secondary antibody Alexa488 or Alexa594 (1:500 or 1:1000 dilution) in 5 % goat serum was added to the cells and incubated for 1 h at RT in the dark. 3 washes with PBS followed. Finally, cells were imaged.

2.8. Western blot

Cell lysates were harvested in the presence or absence of (N-Ethylmaleimide) 25 mM NEM and 25–50 μg protein samples were loaded on a 10 % SDS-PAGE gel. The proteins were then transferred to a PVDF membrane, then blocked using 10 % blocking buffer (10 % milk in PBST) for 1 h at RT. Customized anti-DPPA4 rabbit antibodies were diluted (1:1000) in 5 % blocking buffer and added to the membrane for 1 h and subjected to mild shaking at RT or overnight at 4 °C. Then the membranes were washed 3 times with PBST and probed with anti-rabbit HRP-linked secondary antibody (1:5000 dilution) in 5 % blocking buffer for a 1 h and subjected to mild shaking at RT. The membrane was developed with an ECL reagent (ThermoFisher) in the dark and signals were detected using ImageQuant LAS 4000 series.

2.9. Cellular fractionation

Approximately 4×10^7 cells were washed with PBS buffer, spun and resuspended in 5 volumes of Cytoplasmic Extract (CE) Buffer with NP40 (10 mM, HEPES, 60 mM KCl, 1 mM EDTA, 0.075 % (v/v) NP40, 1 mM DTT and 1 mM PMSF, adjusted to pH 7.6) followed by incubation on ice for 3 min. Then centrifugation using a microcentrifuge at 1000–1500 rpms for 4 min. CE was removed from the pellet into a fresh tube. Nuclei were washed with 100 μl of CE buffer without detergent. Nuclei were spun at 1000–1500 rpms for 4 min and 1 pellet volume of Nuclear Extract (NE) buffer (20 mM Tris Cl, 420 mM NaCl, 1.5 mM MgCl2, 0.2 mM EDTA, 1 mM PMSF and 25 % (v/v) glycerol, adjusted to pH 8.0) was added. The salt concentration was adjusted to a concentration of 400 mM by adding ~35 μl of 5 M NaCl. An equal volume of NE buffer was added and extract was incubated 10 min on ice. CE and NE were spun at maximum speed for 10 min to pellet any nuclei. The contents of the CE tube and NE tube were transferred separately to clean tubes. Glycerol was added to the CE tube to 20 %. Store at − 80 °C.

2.10. Co-immunoprecipitation

The IP were carried out according to the manufacturer's protocol using the PureProteome Protein G magnetic beads (Sigma). Briefly, cells of a 10 cm dish were lysed (20 mM Tris HCl pH 8, 137 mM NaCl, 1 % NP-40, 2 mM EDTA) and DPPA4 antibodies were added to the cell lysates slowly rotating overnight at 4 °C. Then 50 μl Protein G magnetic beads were added for 30 min at RT. Subsequently, the tube was transferred onto the magnetic rack and the supernatant was discarded. The tube was removed from the magnetic rack and the pellet was resuspended in

washing buffer (10 mM Tris; adjust to pH 7.4, 1 mM EDTA, 1 mM EGTA; pH 8.0, 150 mM NaCl, 1 % Triton X-100, Protease inhibitor cocktail). Washing step was repeated twice. Co-immunoprecipitation complexes were eluted by heating beads in 50 µl of 2 x SDS loading buffer without DTT for 10 min at 50 °C. Beads were pelleted and supernatant were transferred to a new tube and DTT (100 mM) added. For 2nd and 3rd elution repeat twice and run on SDS-PAGE for examination.

2.11. Proteomics analysis

For each sample, 100 µg total IP protein complex was subjected to in-solution tryptic digestion. Briefly, IP Proteins were denatured in 0.1 % RapiGest SF at 80 °C for 15 min, reduced in 10 mM Dithiothreitol (DTT) at 60 °C for 30 min, and alkylated in 10 mM Iodoacetamide (IAA) (1.0 µl IAA/10 µl) in the dark for 40 min at RT. Samples were trypsin-digested overnight at 37 °C and were diluted with aqueous 0.1 % formic acid prior to LC/MS analysis. Then, label-free quantitative 1-dimensional Nano Acquity liquid chromatography tandem mass spectrometry on Synapt G2 (Waters, Manchester, UK) was used to generate differential expression proteomics data between the sample groups. Data acquisition using ion mobility separation experiments ($HDMS^E$) were performed over a range of m/z 50–2000 Da for 115 min acquisition time. All samples were analyzed in triplicate runs using the MassLynx programs (version. 4.1, SCN833; and Progenesis QI for proteomics (Progenesis QIfp version 3, Waters/Nonlinear Dynamics, UK) were used for all automated data processing and database searching. The generated peptide masses were searched against the unified (Uniprot/SwissProt non-redundant database www.uniprot.org).

3. Results

3.1. Generation of anti-DPPA4 antibodies

To study the function of human DPPA4, four customized peptide antibodies, AB1, AB2, AB3 and AB4, were generated. To validate these antibodies, immunofluorescence (IF) experiments were carried out, with and without peptide pre-absorbtion, on DPPA4-EGFP fusion-protein-transfected and non-transfected NTERA2 and Human Embryonic Kidney (HEK) cells (Fig. 1A, B, Supplemental Fig. 1–5). The signals of anti-DPPA4 antibodies, AB1 and AB3, were abolished in the presence of the peptides against which they were raised (Fig. 1A, Supplemental Fig. 1, 5). In fact, the peptide block of AB1 was so efficient that elevated DPPA4 levels in DPPA4-EGFP transfected cells were also not detected using an Alexa594 conjugated secondary antibody (Fig. 1A). Further, IF with AB1 co-localized with DPPA4-EGFP signals (Fig. 1A, Supplemental Fig. 1). AB1 was also tested on HEK cells, which do not express DPPA4, and no unspecific binding was detected (Supplemental Fig. 2). However, when HEK cells were transfected with the DPPA4-EGFP fusion construct, the EGFP signals co-localized with AB1 signals (Supplemental Fig. 4). Taken together, the AB1 antibody specifically detects DPPA4. Peptide blocking failed completely to abolish the signals generated by AB4 (data not shown) and partially those generated by AB2 (Supplemental Fig. 1). DPPA4-EGFP overexpressing cells showed no co-localization with the Alexa594 signals, indicating specificity of AB2, but we could still observe strong Alexa594 signals. A plausible explanation could be that AB2, although specifically recognizes DPPA4, also detects (an)other antigen(s), in particular since it is a poly-clonal antibody. However, it did not bind antigens in HEK cells (Supplemental Fig. 2). Taken together, we excluded antibodies AB2 and AB4 from further IF experiments. Signals detected using AB3 were abolished upon peptide block, strongly indicating that AB3 is specific (Supplemental Fig. 5A). Notably, the AB3 antibody displayed cytosolic signals, which were diffused and appeared as clouds, but others were focused, termed cytosolic foci (CF) (Fig. 1B). Indeed, embryonal carcinoma cells, NTERA2 cells and 2102Ep cells and the iPSC IMR90–4 displayed these cytosolic patterns upon DPPA4-EGFP transfection as well (Figs. 1A, B, 2C, D). We also determined the specificity of the antibodies in Western blots and found that AB1, AB3, and AB2 were specifically blocked by the peptides, abolishing the expected DPPA4 band of ~33.5 kDa (Fig. 1C, D, Supplemental Fig. 5–7). AB4, however, was not affected by peptide blocking (data not shown), and, therefore, excluded also from further studies in Western blots. AB1, AB2 and AB3 were also tested on lysates of transgenic DPPA-EGFP NTERA2 and 2102Ep cell lines and the expected upshifted band of ~60 kDa was also abolished, thereby, further substantiating the specificities of these antibodies in Western blots (Supplemental Figs. 5–7). Neither AB1 nor AB2 detected the expected ~33.5 kDa DPPA4 band in HEK cells, which to the best of our knowledge do not express DPPA4, strongly indicating that these antibodies do not bind non-specific in Western blotting (Supplementary Figs. 6 and 7).

Noteworthy, AB1 and AB3 detected an additional unexpected band migrating at ~50 kDa, which was also specifically abolished upon peptide blocking, indicating that a sub-population of DPPA4 might be covalently linked to another factor (Fig. 1C and Supplemental Figs. 5–7).

3.2. DPPA4 sub-cellular localization

We carried out cellular fractionations to determine whether the different sub-cellular localizations correspond to the different DPPA4 bands and potentially to establish a relationship to the observed cytoplasmic population of DPPA4 (Fig. 1E). Indeed, we found that the ~33.5 kDa band corresponds to the nuclear fraction and the ~50 kDa band to the cytoplasmic fraction (Fig. 1E). We also detected bands in the concentrated NE fraction, a ~75 kDa and a band between ~120–130 kDa in size. It was recently reported that DPPA4 is SUMOylated multiple times (>120 kDa, ~100 kDa, ~78 kDa, ~ 60 kDa) determined by the application of ML-792, a specific inhibitor of SUMOylation (Theurillat et al., 2020). However, the authors also showed a band at ~50 kDa, which was unaffected and of equal intensity of the ~100 kDa SUMOylated DPPA4 band. To test whether our observed ~50 kDa band is a SUMOylated version of DPPA4, we carried out an alternative approach. We harvested our protein extracts in the presence and absence of N-Ethylmaleimide (NEM), which preserves SUMO modifications upon cell lysis via inhibition of SENPs, reviewed in Xiao et al. (2015). We also doubled the concentration of antibodies, AB1 and AB2, from 1:1000–1:500 to ensure to detection of potential weaker DPPA4 populations. We did not observe a significant difference in the intensity of the ~50 kDa band in the presence or absence of the NEM inhibitor, suggesting that this band is not a SUMOylated version of DPPA4 (Fig. 1C). However, we did observe a decreased intensity of the ~33.5 kDa band in the presence of NEM, perhaps SUMOylation destabilizes DPPA4 in cooperation with the ubiquitination machinery. Consistent with our previous results, we did not observe the ~50 kDa band with AB2, neither in the presence nor in the absence of NEM, and despite the higher antibody concentration (Fig. 1D, Supplementary Fig. 8). However, we did observe the ~75 kDa band with AB2 that we detected with AB1 in the nuclear fraction (Fig. 1E). This band is indeed specific as it disappears using peptide block, but does not change with or without NEM (Fig. 1D), in contrast to the report of Theurillat and colleagues (Theurillat et al., 2020).

We re-visited the DPPA4-EGFP transfections and quantified the cells that exhibited only nuclear and cells that exhibited both, nuclear and cytosolic signals (Fig. 1F). More than 88 % were nuclear and cytosolic, while almost 12% were nuclear only. Noteworthy, our dismissed AB2 did show similar CFs amongst other non-specific signals (Supplementary Fig. 1).

Retinoic acid (RA) treatment induces neural differentiation of NTERA2 cells, which caused the intensity of the nuclear band to decrease steadily, the cytosolic band, however, increased transiently before it finally decreased. This phenomenon of initial increase was confirmed by RA treated DPPA4-EGFP transfected cells (Fig. 2A, B). Time-laps experiments on diverse human pluripotent stem cell lines, including H7 and IMR90–4 revealed that some of the CF were dynamic,

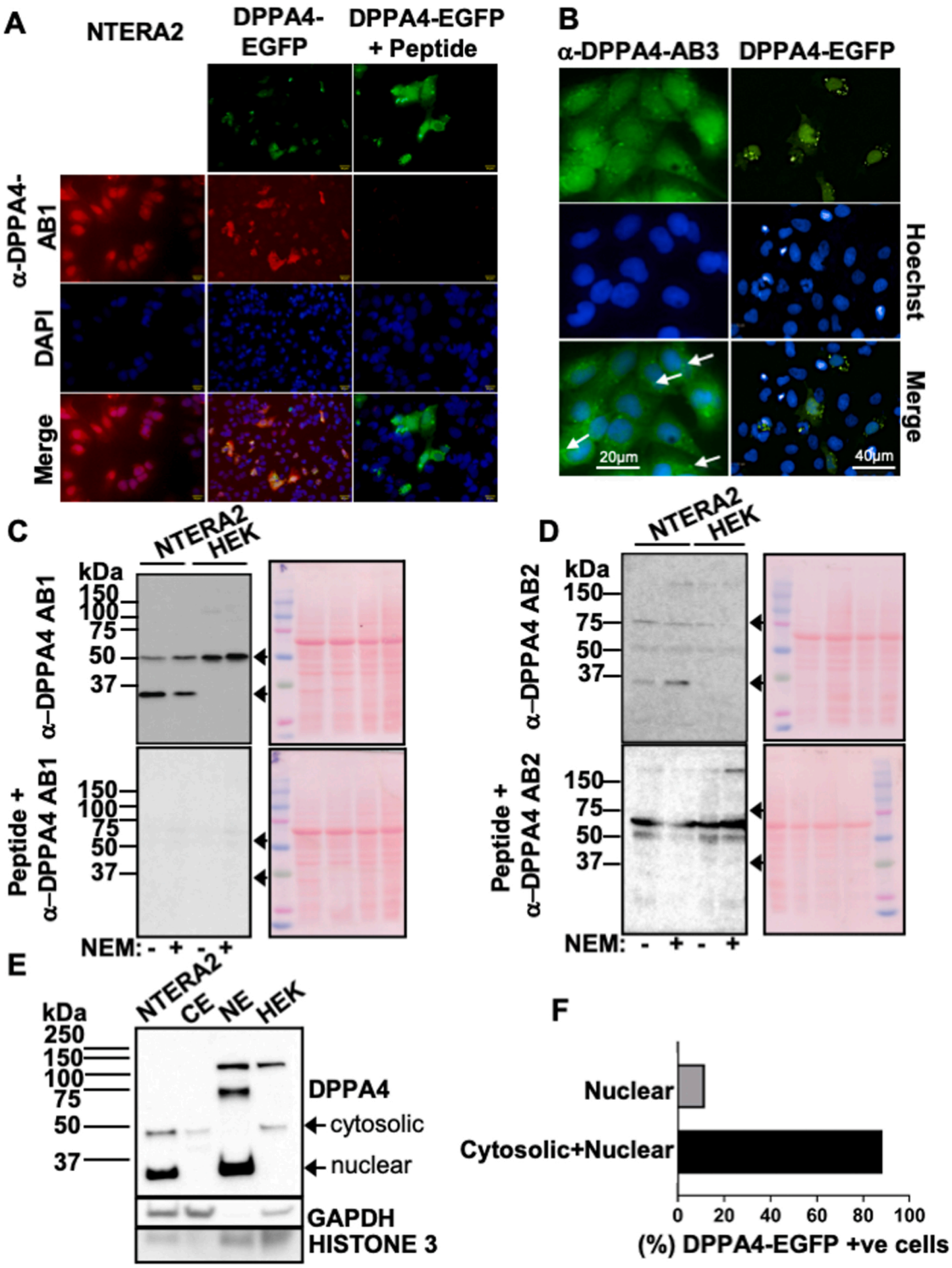

Fig. 1. Sub-cellular localization of DPPA4 and validation of antibodies, AB1, AB2 and AB3, using NTERA2 and HEK cells. A) Antibody peptide block experiments in immunostainings to determine specificity of the AB1 antibody on coverslips. B) Immunostaining in NTERA2 cells using AB3 (left). Arrows indicate CF. DPPA4-EGFP transfected IMR90–4 cells (right). C) Validation of antibody AB1 in Western blot. D) Validation of antibody AB2 in Western blot. In C) and D), left panels Western blots, right panels Ponceau loading controls. Upper blots using antibodies only, lower blots antibodies + peptides. Cells were also harvested in the presence and absence of NEM to assess for SUMOylation. Arrows indicate the specific bands that are abolished upon peptide blocking. E) Cellular fractionation demonstrating that the ~50 kDa band is cytosolic when probed with AB1. Probing with GAPDH and HISTONE serve as loading control and to show the validity of the fractionation. NE= nuclear extract, CE= cytoplasmic extract. Noteworthy, the nuclear extract contains the higher bands observed in C), which is in agreement with the SUMOylation in Theurillat et al. (2020). Also of note, it appears that HEK cells do express modified versions of DPPA4, but not unmodified DPPA4. F) Quantification of DPPA4-EGFP positive (+ve) cells that display cytosolic & nuclear vs nuclear only localization, n = 600.

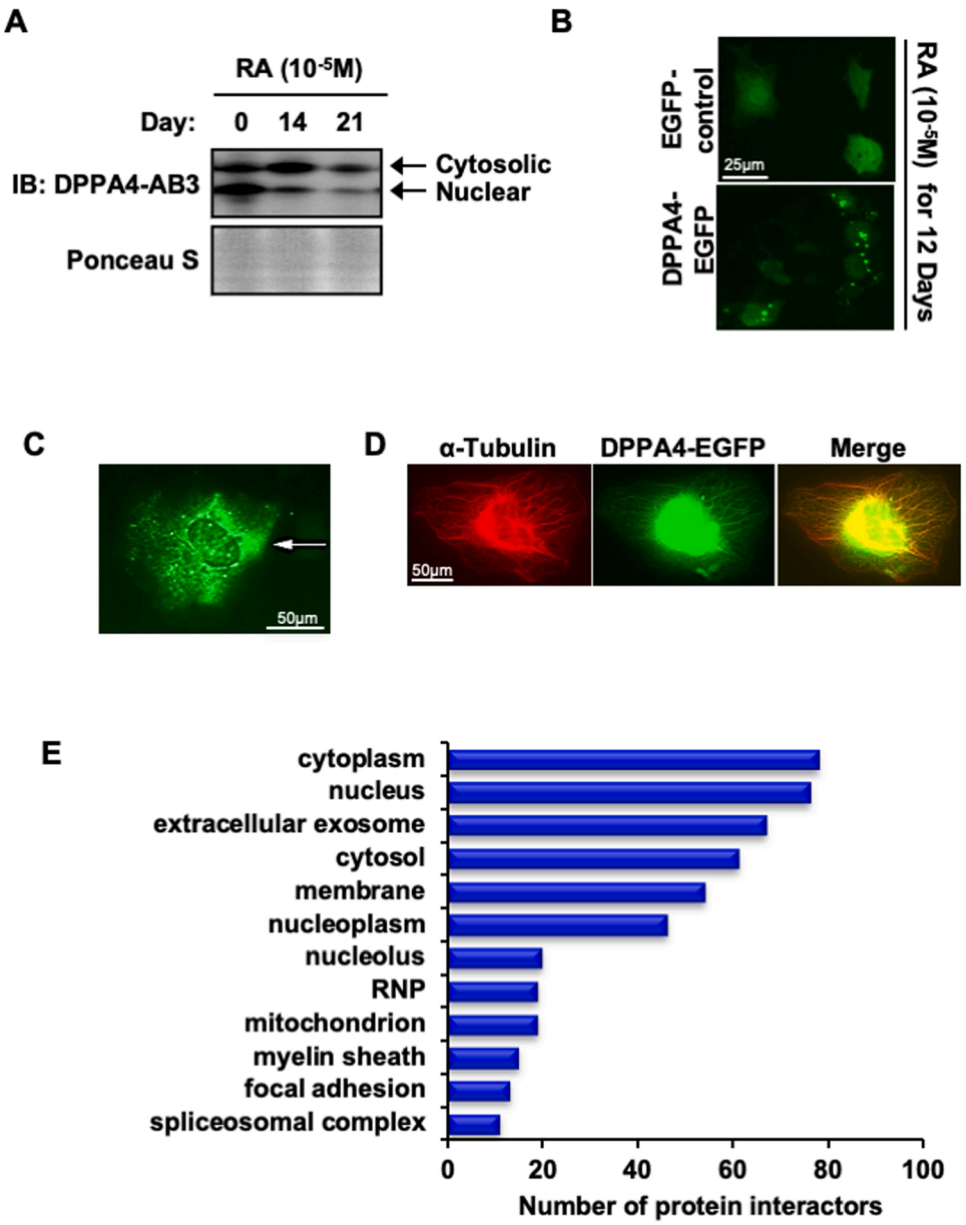

Fig. 2. Differentiation dependent sub-cellular localization of DPPA4 and its interactors. A) Western blotting of RA treated NTERA2 cells using AB3 showed that upon differentiation the 33.5 kDa band decreases, while the 50kda band transiently increases before it finally decreases over 14 and 21 days. B) RA treatment of DPPA4-EGFP transfected vs pCAG-EGFP parental vector control in NTERA2 cells. The nuclear DPPA4-EGFP signals are diminishing while the CFs are not. C) DPPA4-EGFP transfected in 2102Ep cells displaying signals appearing like MTOC (arrow). D) Co-localization of immuno stained α-TUBULIN with DPPA4-EGFP transfected 2102Ep cells. E) Sub-cellular distribution of DPPA4 interacting partners.

and some of those were shuttling between the cytosol and the nucleus (Movies S1–5 in NTERA2 cells). These movies are representative of the processes underlying CF dynamics and may not reflect a quantification of nuclear vs nuclear and cytosolic localization as shown in Fig. 1F. We did not detect any CF in the ER, the Golgi-apparatus, mitochondria, lysosomes, early or late endosomes and microvesicles. However, occasionally the cytosolic DPPA4-EGFP signals were organized in fibrillar spaghetti-like structures (Movies S2, S3, S5), and a few times of these occasions they appeared like microtubuli organizing centers (Fig. 2C). Indeed, immunofluorescence for α-TUBULIN staining on DPPA4-EGFP transfected cells showed the co-localization of both signals (Fig. 2D, Supplemental Fig. 9). Taken together, these results strongly suggest that DPPA4 is present in the cytosol in addition to its known nuclear localization.

Supplementary material related to this article can be found online at doi:10.1016/j.tice.2022.101893.

3.3. Cytosolic interactors and knock-down of DPPA4

To identify cytosolic protein interactors of DPPA4, co-immunoprecipitation (co-IP)/mass-spectrometry using AB1 and AB2 in NTERA2 cells were carried out. These co-IPs were performed in the presence and absence of SUMOylase inhibitor (SUMOyi) NEM to ensure the detection of any SUMO dependent interactions. Proteins that were also identified by the Protein G controls were disregarded. Among the identified interactors was TUBULIN and other previously known interactors like LIN28, PARP1, DDX1, DAZAP1, HNRNPDL, LRRC47, ILF3, CDC5L Histones and DPPA4 itself (Somanath et al., 2018), re-assuring the validity of the experiments (Table S1). We did not pull-down DPPA2 indicating that our co-IP was not saturated. 40 interactors were pulled-down with the AB1 antibody, and approx. double, 82, in the presence of NEM. Also, in the presence of NEM, AB2 pulled-down 85 interactors as opposed to AB2 only, which pulled-down 25 interactors. In total, 232 interactors were detected of which 121 are unique interactors after removing multiple detections (Table S1). Gene ontology enrichment analysis using the DAVID database revealed that 61 of the 121 total DPPA4 interactors are cytosolic, 76 interactors are nuclear, while 38 interactors are found in both compartments (Fig. 2E, Supplementary Table S1). 77 interactors are “poly(A) RNA binding”, 17 are implicated in “mRNA splicing via splicosome” and 12 interactors

function in "protein stability". The four different pull-down conditions, namely the two antibodies, AB1 and AB2, each recognizing different epitopes, in the presence and absence of the SUMOyi, resulted in common, but also different interactors that were pulled-down (Venn diagram in Table S1). Notably, cytoplasmic stress granules, cytoskeletal association and mitochondrial organization were highlighted as well as clathrin-coated pit and cytoskeletal proteins. Indeed, this is substantiated by the observation of our *DPPA4* knock-down experiments. Its depletion in NTERA2 cells resulted besides the exit of self-renewal in the accumulation of vesicles/vacuoles (Fig. 3A-D). The latter indicates a disruption of vesicle/organelle cycling. The success of the *DPPA4* knock-down was monitored by determining the transfection efficiency employing fluorescent cell analysis, semi-quantitative PCR and Western blotting (Supplemental Figs. 10,11). *OK(a)* encodes the TRA1–85 antigen on the cells surface, and was used as a RNAi control gene. It was anticipated that its depletion has no effect on the pluripotent state. Taken together, ~50% of the DPPA4 protein interaction partners are present in the cytosol and the knock-down resulted in a cytosolic phenotype of vesicle biology disruption.

4. Discussion

We demonstrate using custom generated and validated anti-DPPA4 antibodies that in addition to its nuclear localization, DPPA4 is also localized in the cytosol, as diffused clouds, in spaghetti-like structures, and most prominently in shape of CFs. These CFs are mobile, and shuttle between the cytosol and nucleus. We also show that DPPA4 interacts with cytoskeletal elements, mRNA processing proteins, and other cytosolic factors. The significance of this observation is that it paves the way to extend the limited understanding of DPPA4′s critical role in pluripotent stem cells, which in turn are very promising for regenerative therapies.

In addition to the commonly known and expected human DPPA4 band of 33.5 kDa in Western blots, we detected another specific band of ~75 kDa, which was abolished upon peptide blocking. This is in agreement with a recent report of Theurillat and colleagues (Theurillat et al., 2020). In contrast to this report, however, none of these specific bands was altered in the presence of NEM indicating that they are not SUMOylated (Theurillat et al., 2020). This discrepancy is perhaps due to the different methods used, in particular the inhibitors used to disable SUMOylation (ML-792) as opposed to disabling de-SUMOylation (NEM). Another reason could be that the antibodies recognize different epitopes, which would mean that the different results between our study and the report by Theurillat et al. regarding the ~75 kDa band imply a SUMOylated and a non-SUMOylated population of DPPA4 migrating at similar levels in SDS-PAGE. It could also be explained by species differences between the murine and human DPPA4 proteins as mentioned above. Indeed, human DPPA4 is composed of 304 amino acids and it migrates as expected at around ~33.5 kDa, and although murine DPPA4 is 8 amino acids shorter, it migrates at approximately ~42 kDa as opposed to its calculated size of approximately ~32.7 kDa, strongly suggesting species differences on post-translational level beyond mere

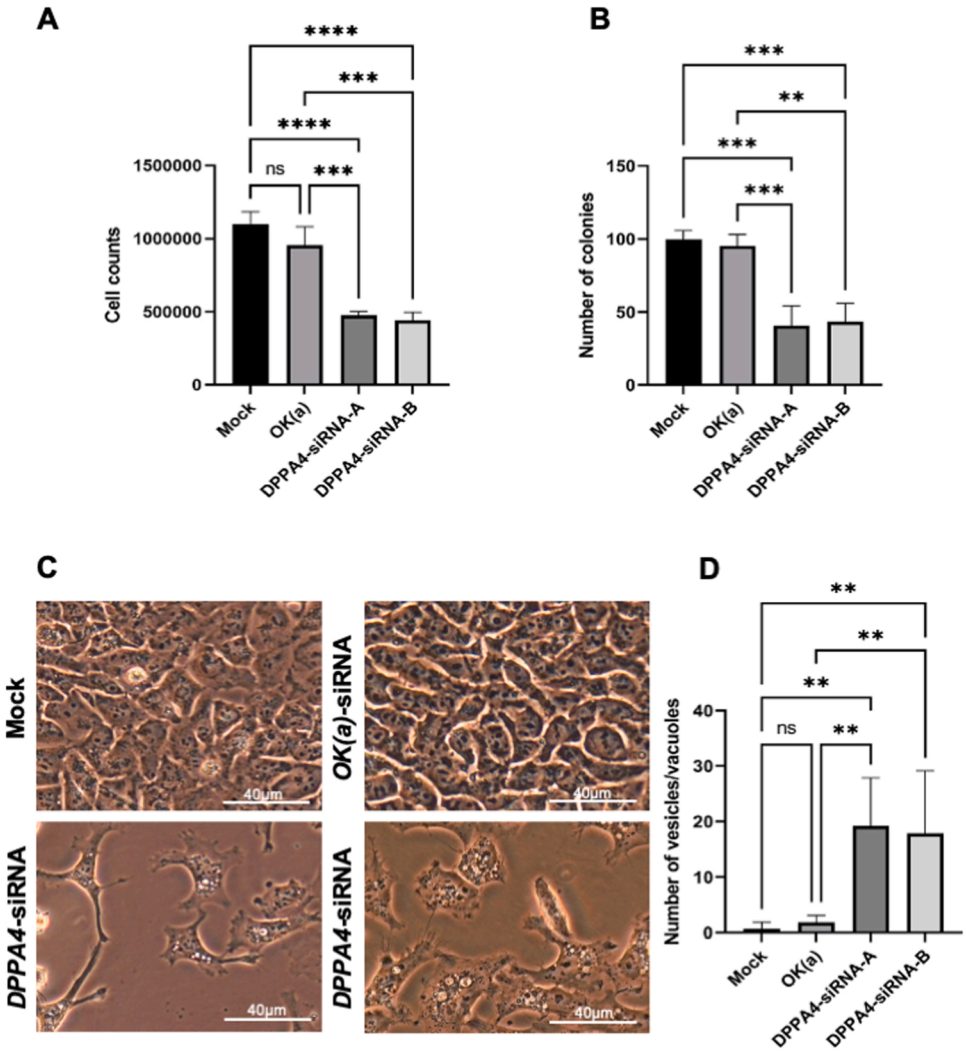

Fig. 3. Knock-down of DPPA4 in NTERA2 cells leads to the exit of self-renewal and accumulation of vesicles/vacuoles. A) 2×10^5 cells were seeded in a 6 well plate and counted 3 days post-transfection. The DPPA4 depleted cells displayed significantly less cell numbers. Statistical analysis using One-Way Anova yielded p-values: *** >0.0005, **** > 0.0001. B) For the cologenicity assay cells were transfected like in A) and 3 post-transfection, cells were trypsinized, and 10,000 cells re-seeded at very low density in a T25 to count the colonies app 7–10 days later. The DPPA4 depleted cells formed significantly less colonies. Statistical analysis using One-Way Anova yielded p-values: ** > 0.0015, *** >0.001. C) Morphology of NTERA2 cells 3 day post-transfection. Prominent vesicles/vacuoles apparent in DPPA4 knock-down cells of DPPA4. D) Quantification of vesicles/ vacuoles observed upon DPPA4 knock-down, p-Value > 0.005.

phosphorylation, since DPPA4 amongst many pluripotency factors was found to be phosphorylated (Zoumaro-Djayoon et al., 2011). More than doubling the protein band size to ~75 kDa is unlikely to be explained only by phosphorylation and probably extends to other modifications like ubiquitylation, neddylation, etc, and maybe even covalent linkage to other factor(s). Anyhow, this issue needs to be addressed experimentally.

4.1. Cytosolic localization of DPPA4

The most important finding of this study, however, is that we found DPPA4 to be localized in the cytosol besides the nucleus. DPPA4′s cytosolic localization has escaped the scientific communities' attention possibly due to the expectation of DPPA4′s sole nuclear presence based on its proven binding to chromatin, DNA and Histones and, hence, its epigenetic role (Hernandez et al., 2018; Engelen et al., 2015; Masaki et al., 2007, 2010; Li et al., 2020; Theurillat et al., 2020; Gretarsson and Hackett, 2020; Lim and Meshorer, 2020; Eckersley-Maslin et al., 2019; Yang et al., 2020; Klein et al., 2018; Zaidan et al., 2018; Dehghanian et al., 2019; Oliviero et al., 2015; Nakamura et al., 2011; Eckersley-Maslin et al., 2020). Any cytosolic signals, mostly CFs, but also non-expected Western blot bands, might have been mistaken as artefacts, background or non-specific. Indeed, commercial available antibodies like R&D systems (cat#AF3730), Thermofisher (cat#PA5–83266), (cat#PA5-23444), (cat#PA5-47530) and academic publications, i.e., in Fig. 1 and 5 (Masaki et al., 2007), Fig. 2 (Maldonado-Saldivia et al., 2007), Fig. 5A (Madan et al., 2009), Fig. 7 in Xenopus (Siegel et al., 2009), Figs. 1, 2 and 7 (Masaki et al., 2010), Fig. 7 (Nakamura et al., 2011) show similar structures like our reported CFs and sometimes a higher and additional band in Western blots. As an example, the ~50 kDa band in Masaki et al. is annotated as unspecific (Masaki et al., 2007). In another report, the authors show in Fig. 5b only the expected band, and in the Extended Figs. 1a and 2d they do not comment on the additionally detected higher band (presumably ~50 kDa) (Eckersley-Maslin et al., 2020). We presume that there are even more apparent images in many studies, which were, however, not included because they were mistaken as artefacts. Also, it is known that different antibodies differ in signal detection in particular poly-clonal antibodies. Given the above and together with the results of our study, the previously overlooked ~50 kDa band appears to be real and is common to the human and murine system in spite of species differences regarding the calculated and expected band.

The ~50 kDa band is specific as it was abolished by peptide competition. It was also not SUMOylated, because NEM, a SUMOylase inhibitor, had no effect. This is in agreement with the report by Theurillat and colleagues, who used a complementing approach by employing a SUMOylation inhibitor instead of SUMOylase inhibitor, and also did not show any effect, however, a band that was not highlighted or discussed (Theurillat et al., 2020). Therefore, the ~50 kDa band might be another post-translational modification like phosphorylation, ubiquitylation, neddylation, etc. Another plausible explanation could be that ~50 kDa might be a splice variant. However, no such splice variants has been predicted by the genomic databases. Further studies are required to clarify this issue.

Noteworthy, we detected the ~50 kDa band in HEK cells, but not the 33.5 kDa band commonly found in human pluripotent stem cells, which might indicate that somatic cells do express the cytosolic form of DPPA4, which could be in agreement with our observation that upon differentiation DPPA4 is exported from the nucleus into the cytosol.

The cellular fractionations using AB1 showed that the ~50kD band is in the cytoplasmic extract. We failed to detect any CF in the ER, the Golgi-apparatus, mitochondria, lysosomes, early or late endosomes and microvesicles. However, it was co-localized with α-TUBULIN and more than 60 identified DPPA4 interaction partners were cytosolic. We conclude, therefore, that these dynamic DPPA4 foci, the spaghetti-like structures and clouds are cytosolic.

4.2. Cytosolic interaction partners of DPPA4 and potential functions

The DPPA4 interaction partners strongly indicate that it might be involved in the regulation of gene expression at mRNA level (processing/RNA transport), which is in agreement with other SAP domain proteins (Aravind and Koonin, 2000). Indeed, Knoepfler and colleagues have also shown that a large proportion of DPPA4 protein interactors are cytosolic and bind RNA (Somanath et al., 2018). DPPA4 CF appear similar to other cytosolic foci like cytoplasmic foci, stress granules, U-bodies, P-bodies and C-bodies, and might therefore also be implicated in RNA decay, mRNA storage sites or pre-mRNA processing (van Dijk et al., 2002; Cougot et al., 2004; Baguet et al., 2007; Liu and Gall, 2007; Liu et al., 2005; Sheth and Parker, 2003; Brengues et al., 2005; Kotaja and Sassone-Corsi, 2007; Kotaja et al., 2006). Finally, the co-IPs in the presence and absence of the SUMOylase inhibitor NEM, will most likely affect the potential SUMOylation of all interactors, and thus, their altered properties, including their interaction with each other. Anyhow, we only observed an increased number of interactors, but not different classes of interaction with and without the inhibitor (Table S1).

In an attempt to integrate and understand the various observations the following scenario might be the case. The dynamic DPPA4 CF including cytosolic-nuclear shuttling appear rather regulated than random, since it interacts with elements of the cytoskeleton (α-TUBULIN, β-ACTIN). Covalently modified DPPA4, which increases upon RA mediated differentiation, might be a cargo load, perhaps Histones, which are required for differentiation to be replaced (Barrero et al., 2013) and, thereby exported, following a highly specific route along the cytoskeletal tracks to a pre-determined destination (i.e., mRNA storage sites).

The depletion of *DPPA4* in NTERA2 appeared to disrupt vesicle biology. Indeed, we identified DNM1L, CTTN, HSPD1 (associated with clathrin-coated pits) as interacting partners of DPPA4. Moreover, the endophilins SH3GL1 and SH3GL3 (implicated in endocytosis) have also been previously reported to interact with DPPA4 (Stelzl et al., 2005). Perhaps such functions are in context of intracellular membrane remodelling and/or transport as observed with DPPA2 (Xue et al., 2013). However, maybe this vesicle phenotype is a result of the reduced robustness of NTERA2 towards the manipulation of pluripotent genetic circuits due to its teratocarcinogenic origin. Indeed, such a vesicle phenotype has not been previously observed in mESCs (Ivanova et al., 2006; Hernandez et al., 2018; Nakamura et al., 2011; Madan et al., 2009). It would perhaps be of significant interest to re-examine DPPA4 in other cell lines in the context of our newly identified interactors and pathways.

All of these speculations are supported by the interaction of DPPA4 with Histones (Engelen et al., 2015; Masaki et al., 2010), the dynamic mobility of the CF and shuttling between nucleus and cytosol (movies), the interaction with "nuclear pore complex" proteins, "nuclear import" and "export" like TNPO1, KPNB1, KPNB3, which belong to the karyopherins (importins and exportins). It might not only be that DPPA4 itself is regulated and directed along specific cytoskeletal tracks, but that DPPA4, too, has a cytoskeletal regulatory function. Indeed, our DPPA4 *in silico* analysis, revealed a homology stretch to ARP2/3, an actin polymerization and branching inducer, which might point to a potential actin cytoskeleton regulatory function (Smith et al., 2013; Goley and Welch, 2006) together with our identified protein interaction partner and actin polymerization regulator PROFILIN (Funk et al., 2019; Pantaloni and Carlier, 1993). This is in agreement with the fact that DPPA2, which is co-expressed, co-regulated under the control of the same cis-regulatory elements and is a protein interaction partner of DPPA4, binds to microtubuli to regulate the de-condensation of the heavily compacted sperm heads upon fertilization (Boyer et al., 2005; Nakamura et al., 2011; Maldonado-Saldivia et al., 2007; Siegel et al., 2009; Stelzl et al., 2005; Xue et al., 2013).

Some of these hypotheses could be addressed by subjecting the cytoplasmic fraction, which contains the ~50 kDa population of DPPA4,

to IPs followed by, first, RNA binding and RNA-sequencing assays. Second, to ACTIN cytoskeleton polymerization assays in particular to branching of ACTIN. Third, to protein-sequencing of RA induced and non-induced pluripotent stem cells to determine whether the ~50 kDa population is a post-translational modification, a splice variant of DPPA4 or DPPA4 carrying a cargo (covalent or non-covalent) or not. It might also be useful to carry out secretion and endocytosis assays on DPPA4 depleted and non-depleted pluripotent stem cells to address the vesicle phenotype.

5. Conclusion

DPPA4 and its interactors are not limited to occupy only the nucleus, but they are also localized in the cytosol. Here, DPPA4 appears as spaghetti-like structures, as diffused clouds and as distinct foci. These cytosolic foci (CF) are dynamic, and shuttle between the cytosol and the nucleus. A significant proportion of the cytosolic interactors of DPPA4 are implicated in mRNA processing and RNA and protein transport between the cytosol and the nucleus. DPPA4′s down-regulation upon differentiation dramatically decreases its nuclear presence, and transiently increases its cytosolic presence, before it finally decreases. It appears as if its ~33.5 kDa band is specific to the undifferentiated pluripotency state. Furthermore, the knock-down of *DPPA4* resulted in cytosolic accumulation of vesicles/vacuoles. This study points to new research directions that will shed more light on DPPA4′s multiple functional roles that appear to be critical in mammalian pluripotent stem cells.

Ethics approval and consent to participate

Not applicable.

Funding

by KFSHRC, RAC# 2160-025 and the University of Sheffield.

CRediT authorship contribution statement

Raed Abu-Dawud: Writing – review & editing, Investigation, Supervision, Writing – orignal draft, Writing – review & editing. **Bhavesh V. Mistry:** Investigation, Writing – review & editing. **Renad Almahdali:** Investigation. **Maryam M. Matin:** Investigation, Writing – review & editing. **Ayodele Alaiya:** Investigation. **Fatimah Alghamdi:** Investigation. **Hala Alamari:** Investigation. **Nadya Al-Yacoub:** Investigation, Writing – orignal draft, Writing – review & editing. **Junaid Kashir:** Writing – review & editing. **Marwa Houssein:** Investigation. **Abdullah Alawad:** Resources, Writing – review & editing. **Peter W. Andrews:** Resources, Writing – review & editing, Funding acquisition. **Abdullah M. Assiri:** Resources, Writing – review & editing, Funding acquisition.

Consent for publication

Not applicable.

Competing interest statement

The authors declare no competing interests.

Data Availability

Additional data, antibodies and plasmids are available upon request. The datasets used and/or analysed during the current study are available from the corresponding author on request.

Appendix A. Supporting information

Supplementary data associated with this article can be found in the online version at doi:10.1016/j.tice.2022.101893.

References

Bortvin, A., Eggan, K., Skaletsky, H., Akutsu, H., Berry, D.L., Yanagimachi, R., Page, D.C., Jaenisch, R., 2003. Incomplete reactivation of Oct4-related genes in mouse embryos cloned from somatic nuclei. Development 130 (8), 1673–1680.

Ivanova, N., Dobrin, R., Lu, R., Kotenko, I., Levorse, J., DeCoste, C., Schafer, X., Lun, Y., Lemischka, I.R., 2006. Dissecting self-renewal in stem cells with RNA interference. Nature 442 (7102), 533–538.

Enver, T., Soneji, S., Joshi, C., Brown, J., Iborra, F., Orntoft, T., Thykjaer, T., Maltby, E., Smith, K., Abu Dawud, R., Jones, M., Matin, M., Gokhale, P., Draper, J., Andrews, P. W., 2005. Cellular differentiation hierarchies in normal and culture adapted human embryonic stem cells. Hum. Mol. Genet.

Golipour, A., David, L., Liu, Y., Jayakumaran, G., Hirsch, C.L., Trcka, D., Wrana, J.L., Late, A., 2012. Transition in somatic cell reprogramming requires regulators distinct from the pluripotency network. Cell Stem Cell 11 (6), 769–782.

Hernandez, C., Wang, Z., Ramazanov, B., Tang, Y., Mehta, S., Dambrot, C., Lee, Y.W., Tessema, K., Kumar, I., Astudillo, M., Neubert, T.A., Guo, S., Ivanova, N.B., 2018. Dppa2/4 facilitate epigenetic remodeling during reprogramming to pluripotency. Cell Stem Cell.

Niwa, H., Miyazaki, J., Smith, A.G., 2000. Quantitative expression of Oct-3/4 defines differentiation, dedifferentiation or self-renewal of ES cells. Nat. Genet 24 (4), 372–376.

Chambers, I., Colby, D., Robertson, M., Nichols, J., Lee, S., Tweedie, S., Smith, A., 2003. Functional expression cloning of Nanog, a pluripotency sustaining factor in embryonic stem cells. Cell 113 (5), 643–655.

Mitsui, K., Tokuzawa, Y., Itoh, H., Segawa, K., Murakami, M., Takahashi, K., Maruyama, M., Maeda, M., Yamanaka, S., 2003. The homeoprotein Nanog is required for maintenance of pluripotency in mouse epiblast and ES cells. Cell 113 (5), 631–642.

Ying, Q.L., Nichols, J., Chambers, I., Smith, A., 2003. BMP induction of Id proteins suppresses differentiation and sustains embryonic stem cell self-renewal in collaboration with STAT3. Cell 115 (3), 281–292.

Boyer, L.A., Lee, T.I., Cole, M.F., Johnstone, S.E., Levine, S.S., Zucker, J.P., Guenther, M. G., Kumar, R.M., Murray, H.L., Jenner, R.G., Gifford, D.K., Melton, D.A., Jaenisch, R., Young, R.A., 2005. Core transcriptional regulatory circuitry in human embryonic stem cells. Cell 122 (6), 947–956.

Matin, M.M., Walsh, J.R., Gokhale, P.J., Draper, J.S., Bahrami, A.R., Morton, I., Moore, H.D., Andrews, P.W., 2004. Specific knockdown of Oct4 and {beta}2-microglobulin expression by RNA interference in human embryonic stem cells and embryonic carcinoma cells. Stem Cells 22 (5), 659–668.

Aravind, L., Koonin, E.V., 2000. SAP - a putative DNA-binding motif involved in chromosomal organization. Trends Biochem Sci. 25 (3), 112–114.

Loh, K.M., Lim, B., 2011. A precarious balance: pluripotency factors as lineage specifiers. Cell Stem Cell 8 (4), 363–369.

Engelen, E., Brandsma, J.H., Moen, M.J., Signorile, L., Dekkers, D.H., Demmers, J., Kockx, C.E., Ozgur, Z., van, I.W.F., van den Berg, D.L., Poot, R.A., 2015. Proteins that bind regulatory regions identified by histone modification chromatin immunoprecipitations and mass spectrometry. Nat. Commun. 6, 7155.

Masaki, H., Nishida, T., Kitajima, S., Asahina, K., Teraoka, H., 2007. Developmental pluripotency-associated 4 (DPPA4) localized in active chromatin inhibits mouse embryonic stem cell differentiation into a primitive ectoderm lineage. J. Biol. Chem. 282 (45), 33034–33042.

Masaki, H., Nishida, T., Sakasai, R., Teraoka, H., 2010. DPPA4 modulates chromatin structure via association with DNA and core histone H3 in mouse embryonic stem cells. Genes Cells 15 (4), 327–337.

H. Li, C. Long, J. Xiang, P. Liang, X. Li, Y. Zuo, Dppa2/4 as a trigger of signaling pathways to promote zygote genome activation by binding to CG-rich region, Briefings in bioinformatics (2020).

Thomson, J.A., Itskovitz-Eldor, J., Shapiro, S.S., Waknitz, M.A., Swiergiel, J.J., Marshall, V.S., Jones, J.M., 1998. Embryonic stem cell lines derived from human blastocysts. Science 282 (5391), 1145–1147.

Yu, J., Vodyanik, M.A., Smuga-Otto, K., Antosiewicz-Bourget, J., Frane, J.L., Tian, S., Nie, J., Jonsdottir, G.A., Ruotti, V., Stewart, R., Slukvin II, Thomson, J.A., 2007. Induced pluripotent stem cell lines derived from human somatic cells. Science 318 (5858), 1917–1920.

Andrews, P.W., Damjanov, I., Simon, D., Banting, G.S., Carlin, C., Dracopoli, N.C., Fogh, J., 1984. Pluripotent embryonal carcinoma clones derived from the human teratocarcinoma cell line Tera-2. Differentiation in vivo and in vitro. Lab Invest 50 (2), 147–162.

Andrews, P.W., Bronson, D.L., Benham, F., Strickland, S., Knowles, B.B., 1980. A comparative study of eight cell lines derived from human testicular teratocarcinoma. Int J. Cancer 26 (3), 269–280.

Theurillat, I., Hendriks, I.A., Cossec, J.C., Andrieux, A., Nielsen, M.L., Dejean, A., 2020. Extensive SUMO modification of repressive chromatin factors distinguishes pluripotent from somatic cells. Cell Rep. 32 (11), 108146.

Xiao, Y., Pollack, D., Nieves, E., Winchell, A., Callaway, M., Vigodner, M., 2015. Can your protein be sumoylated? A quick summary and important tips to study SUMO-modified proteins. Anal. Biochem. 477, 95–97.
Somanath, P., Bush, K.M., Knoepfler, P.S., 2018. ERBB3-binding protein 1 (EBP1) is a novel developmental pluripotency-associated-4 (DPPA4) cofactor in human pluripotent cells. Stem Cells 36 (5), 671–682.
Zoumaro-Djayoon, A.D., Ding, V., Foong, L.Y., Choo, A., Heck, A.J., Munoz, J., 2011. Investigating the role of FGF-2 in stem cell maintenance by global phosphoproteomics profiling. Proteomics 11 (20), 3962–3971.
Gretarsson, K.H., Hackett, J.A., 2020. Dppa2 and Dppa4 counteract de novo methylation to establish a permissive epigenome for development. Nat. Struct. Mol. Biol. 27 (8), 706–716.
Lim, P.S.L., Meshorer, E., 2020. Dppa2 and Dppa4 safeguard bivalent chromatin in order to establish a pluripotent epigenome. Nat. Struct. Mol. Biol. 27 (8), 685–686.
Eckersley-Maslin, M., Alda-Catalinas, C., Blotenburg, M., Kreibich, E., Krueger, C., Reik, W., 2019. Dppa2 and Dppa4 directly regulate the Dux-driven zygotic transcriptional program. Genes Dev. 33 (3–4), 194–208.
Yang, L., Liu, X., Song, L., Di, A., Su, G., Bai, C., Wei, Z., Li, G., 2020. Transient Dux expression facilitates nuclear transfer and induced pluripotent stem cell reprogramming. EMBO Rep. 21 (9), e50054.
Klein, R.H., Tung, P.Y., Somanath, P., Fehling, H.J., Knoepfler, P.S., 2018. Genomic functions of developmental pluripotency associated factor 4 (Dppa4) in pluripotent stem cells and cancer. Stem Cell Res. 31, 83–94.
Zaidan, N.Z., Walker, K.J., Brown, J.E., Schaffer, L.V., Scalf, M., Shortreed, M.R., Iyer, G., Smith, L.M., Sridharan, R., 2018. Compartmentalization of HP1 proteins in pluripotency acquisition and maintenance. Stem Cell Rep. 10 (2), 627–641.
Dehghanian, F., Hojati, Z., Esmaeili, F., Masoudi-Nejad, A., 2019. Network-based expression analyses and experimental validations revealed high co-expression between Yap1 and stem cell markers compared to differentiated cells. Genomics 111 (4), 831–839.
Oliviero, G., Munawar, N., Watson, A., Streubel, G., Manning, G., Bardwell, V., Bracken, A.P., Cagney, G., 2015. The variant polycomb repressor complex 1 component PCGF1 interacts with a pluripotency sub-network that includes DPPA4, a regulator of embryogenesis. Sci. Rep. 5, 18388.
Nakamura, T., Nakagawa, M., Ichisaka, T., Shiota, A., Yamanaka, S., 2011. Essential roles of ECAT15-2/Dppa2 in functional lung development. Mol. Cell Biol. 31 (21), 4366–4378.
Eckersley-Maslin, M.A., Parry, A., Blotenburg, M., Krueger, C., Ito, Y., Franklin, V.N.R., Narita, M., D'Santos, C.S., Reik, W., 2020. Epigenetic priming by Dppa2 and 4 in pluripotency facilitates multi-lineage commitment. Nat. Struct. Mol. Biol. 27 (8), 696–705.
Maldonado-Saldivia, J., van den Bergen, J., Krouskos, M., Gilchrist, M., Lee, C., Li, R., Sinclair, A.H., Surani, M.A., Western, P.S., 2007. Dppa2 and Dppa4 are closely linked SAP motif genes restricted to pluripotent cells and the germ line. Stem Cells 25 (1), 19–28.
Madan, B., Madan, V., Weber, O., Tropel, P., Blum, C., Kieffer, E., Viville, S., Fehling, H. J., 2009. The pluripotency-associated gene Dppa4 is dispensable for embryonic stem cell identity and germ cell development but essential for embryogenesis. Mol. Cell Biol. 29 (11), 3186–3203.
Siegel, D., Schuff, M., Oswald, F., Cao, Y., Knöchel, W., 2009. Functional dissection of XDppa2/4 structural domains in Xenopus development. Mech. Dev. 126 (11), 974–989.
van Dijk, E., Cougot, N., Meyer, S., Babajko, S., Wahle, E., Seraphin, B., 2002. Human Dcp2: a catalytically active mRNA decapping enzyme located in specific cytoplasmic structures. EMBO J. 21 (24), 6915–6924.
Cougot, N., Babajko, S., Seraphin, B., 2004. Cytoplasmic foci are sites of mRNA decay in human cells. J. Cell Biol. 165 (1), 31–40.
Baguet, A., Degot, S., Cougot, N., Bertrand, E., Chenard, M.-P., Wendling, C., Kessler, P., Le Hir, H., Rio, M.-C., Tomasetto, C., 2007. The exon-junction-complex-component metastatic lymph node 51 functions in stress-granule assembly. J. Cell Sci. 120 (16), 2774–2784.
Liu, J.-L., Gall, J.G., 2007. U bodies are cytoplasmic structures that contain uridine-rich small nuclear ribonucleoproteins and associate with P bodies. PNAS 104 (28), 11655–11659.
Liu, J., Valencia-Sanchez, M.A., Hannon, G.J., Parker, R., 2005. MicroRNA-dependent localization of targeted mRNAs to mammalian P-bodies. Nat. Cell Biol. 7 (7), 719–723.
Sheth, U., Parker, R., 2003. Decapping and decay of messenger RNA occur in cytoplasmic processing bodies. Science 300 (5620), 805–808.
Brengues, M., Teixeira, D., Parker, R., 2005. Movement of eukaryotic mRNAs between polysomes and cytoplasmic processing bodies. Science 310 (5747), 486–489.
Kotaja, N., Sassone-Corsi, P., 2007. The chromatoid body: a germ-cell-specific RNA-processing centre. Nat. Rev. Mol. Cell Biol. 8 (1), 85–90.
Kotaja, N., Bhattacharyya, S.N., Jaskiewicz, L., Kimmins, S., Parvinen, M., Filipowicz, W., Sassone-Corsi, P., 2006. The chromatoid body of male germ cells: similarity with processing bodies and presence of Dicer and microRNA pathway components. Proc. Natl. Acad. Sci. USA 103 (8), 2647–2652.
Barrero, M.J., Sese, B., Martí, M., Izpisua, J.C., 2013. Belmonte, Macro histone variants are critical for the differentiation of human pluripotent cells. J. Biol. Chem. 288 (22), 16110–16116.
Stelzl, U., Worm, U., Lalowski, M., Haenig, C., Brembeck, F.H., Goehler, H., Stroedicke, M., Zenkner, M., Schoenherr, A., Koeppen, S., Timm, J., Mintzlaff, S., Abraham, C., Bock, N., Kietzmann, S., Goedde, A., Toksoz, E., Droege, A., Krobitsch, S., Korn, B., Birchmeier, W., Lehrach, H., Wanker, E.E., 2005. A human protein-protein interaction network: a resource for annotating the proteome. Cell 122 (6), 957–968.
Xue, J.Z., Woo, E.M., Postow, L., Chait, B.T., Funabiki, H., 2013. Chromatin-bound Xenopus Dppa2 shapes the nucleus by locally inhibiting microtubule assembly. Dev. Cell 27 (1), 47–59.
Smith, B.A., Daugherty-Clarke, K., Goode, B.L., Gelles, J., 2013. Pathway of actin filament branch formation by Arp2/3 complex revealed by single-molecule imaging. Proc. Natl. Acad. Sci. 110 (4), 1285–1290.
Goley, E.D., Welch, M.D., 2006. The ARP2/3 complex: an actin nucleator comes of age. Nat. Rev. Mol. Cell Biol. 7 (10), 713–726.
Funk, J., Merino, F., Venkova, L., Heydenreich, L., Kierfeld, J., Vargas, P., Raunser, S., Piel, M., Bieling, P., 2019. Profilin and formin constitute a pacemaker system for robust actin filament growth. eLife 8.
Pantaloni, D., Carlier, M.F., 1993. How profilin promotes actin filament assembly in the presence of thymosin beta 4. Cell 75 (5), 1007–1014.